Quantum Size Effect Driven Structure Modifications of Bi Films on Ni(111)

Tjeerd R. J. Bollmann, Raoul van Gastel, Harold J. W. Zandvliet, and Bene Poelsema

Physics of Interfaces and Nanomaterials, MESA$^+$ *Institute for Nanotechnology, University of Twente, Post Office Box 217, NL-7500AE Enschede, The Netherlands*

(Received 12 April 2011; published 19 October 2011)

The quantum-size effect (QSE) driven growth of Bi film structures on Ni(111) was studied *in situ* using low energy electron microscopy and selective area low energy electron diffraction (μLEED). Domains with a (3×3), $\begin{bmatrix} 3 & -1 \\ 1 & 2 \end{bmatrix}$, and (7×7) film structure are found with a height of 3, 5, and 7 atomic layers, respectively. A comparison of I/V-μLEED curves with tensor LEED calculations shows perfectly accommodated Fermi wavelengths, indicative that not only the quantized height, but also the film structure is driven by QSE.

DOI: 10.1103/PhysRevLett.107.176102 PACS numbers: 68.55.J−, 68.37.Nq, 73.21.Fg

The structure and morphology of thin metal films can alter the physical properties of a material so that they become different from those of the bulk material. This can be a result of, e.g., film structure and/or the usually disregarded QSE. For thin Bi (a prototype group V semimetal) films these effects can play a dominant role in determining the film structure, since its electronic properties are a result of the tiny overlap between the valence and conduction bands. The films therefore balance between being a metal or semiconductor [1]. A rather unusual growth mode that has a profound influence on thin film morphology, can occur due to the QSE and is referred to as quantum or electronic growth. QSE's give rise to specific preferred film heights as the result of a characteristic relationship between the Fermi wavelength and the interlayer spacing [2–4]. Thin Pb(111) films are the main representative of this class of materials since their bilayer increment almost perfectly accommodates $3/2$ Fermi wavelengths, resulting in a quasi bilayer oscillation of the thin film stability and its physical properties [5]. Bulk Bi is very similar to Pb since the Fermi energy calculated from a free electron model of bulk Bi is only 0.43 eV higher [6]. The slight structure distortion along the trigonal axis of bulk Bi is however known to cause the band structure to become semimetallic. This results in exotic properties such as long (er) Fermi wavelengths [7]. Besides that, Bi is also a soft semimetal, making electronic effects more pronounced than strain effects. This property makes thin Bi films prime candidates for allotropism. For Bi on Ni(111), a (7×7) and $(\sqrt{7/4} \times \sqrt{7/4}) - R19°$ overlayer structure was found in literature [8]. From a straight forward textbook free electron calculation, the (7×7) overlayer structure should be able to accommodate $3/2$ Fermi wavelength (within 10%) in a bilayer increment as well. Deposition on a suitable substrate therefore makes Bi a candidate for electronic growth, as we will show in this Letter.

Here, we present a study that investigates the growth of thin Bi domains on Ni(111) at temperatures ranging from 423 K up to 474 K. Using *in situ* low energy electron microscopy (LEEM) and low energy electron diffraction μLEED we are able to probe the properties and ordering of different Bi film structures. Our observations show that the structure of the domains that grow is driven by the QSE that results from the accommodation of $n/2$ Fermi wavelengths.

The experiments were performed in an Elmitec LEEM III instrument. A Ni(111) single crystal was cleaned by cycles of 1 keV Ar^+ bombardment at room temperature, followed by flash annealing to a temperature of 1150 K. The cleanliness of the sample was monitored using Auger electron spectroscopy and LEEM. LEEM images revealed an average step-step separation of $\sim$1 μm. All sample temperatures are within an error bar of 6% and were calibrated using the uphill motion of steps over time at a temperature where sublimation is expected, as described in Ref. [9]. Bismuth was deposited from a Knudsen cell.

To determine the properties of the first Bi layer on top of the Ni(111) surface we performed μLEED illuminating a circular area of 1.4 μm diameter during growth at 474 K. A $(\sqrt{3} \times \sqrt{3}) - R30°$ surface alloy shows its maximum peak intensity at a coverage of 0.33 ML (where 1 ML corresponds to 1 Bi-atom per Ni surface atom), in agreement with literature [8,10–12]. Dealloying then leads to the creation of a wetting layer and peaks associated with an incommensurate Bi overlayer appear in the μLEED moiré pattern at a coverage of 0.45 ML. These Bi peaks shift outwards with increasing coverage, indicating a continuous in-plane compression of the lattice constant, yielding an incommensurate Bi film until a stable commensurate (7×7) surface structure locks in. The latter forms when the lattice constant (3.50 Å) stabilizes and was used for an exact *in situ* calibration of the deposition rate. The measured rate is identical to that obtained from the maximum peak intensity for the $(\sqrt{3} \times \sqrt{3}) - R30°$ surface alloy. The Bi (7×7) wetting layer structure, known from literature [8], has a unit cell of 25 Bi atoms.

After completion of the wetting layer, Bi nanowires appear with an orientation that is threefold symmetric,

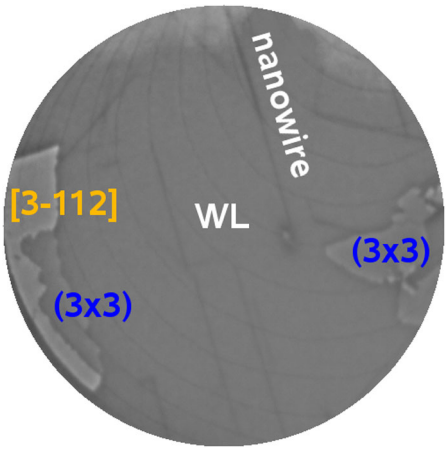

FIG. 1 (color online). LEEM image of a (3 × 3) domain and a [3-112] domain, both surrounded by the (7 × 7) wetting layer. The field of view (FoV) is 10 μm, the electron energy is 20 eV, the substrate temperature is 474 K and the Bi coverage $\theta_{\mathrm{Bi/Ni}} = 0.66$ ML.

see Fig. 1. The details of these wires are discussed elsewhere [13]. From a coverage of 0.51 ML onward two different domains appear, as is illustrated by Fig. 1. μLEED reveals the domain structures to be (3 × 3) and

$$\begin{bmatrix} 3 & -1 \\ 1 & 2 \end{bmatrix}.$$

The LEED patterns and unit cells are shown in Figs. 2(b), 2(c), 2(e), and 2(f), respectively. The in-plane lattice constants of these film structures are 3.74 Å and 3.80 Å at single layer coverages of 0.444 and 0.429 ML, respectively. For convenience we will write the matrix as [3-112]. Both types of domains grow at an anomalously low rate, suggesting that the domains are substantially higher than one atomic layer. An estimate of the heights can be obtained by comparison to the Bi deposition rate. Describing the total coverage ($\theta_{\mathrm{Bi/Ni}}$) as the sum of the fractional areas (ϕ_i) corresponding to the different film structures times their respective layer coverage (θ_i), one can calculate the average height of the domains using the relation:

$$\begin{aligned}\theta_{\mathrm{Bi/Ni}} &= \sum_i \phi_i \theta_i \\ &= \phi_{\mathrm{WL}} \times 0.510 + \phi_{[3-112]} \times 0.429 \times n_{[3-112]} \\ &\quad + \phi_{(3\times3)} \times 0.444 \times n_{(3\times3)},\end{aligned}$$

where $n_{(3\times3)}$ and $n_{[3-112]}$ are the number of atomic layers of the two film structures. The (3 × 3) domains occur more abundantly than [3-112] domains and several measurements of the exclusive growth of (3 × 3) domains reveal an average height of 3.0 ± 0.1 atomic layers. In a similar manner an average height of 5.1 ± 0.2 atomic layers is found for the [3-112] domains. From conservation of the amount of deposited material, we can also derive that both the (3 × 3) and [3-112] film structures grow directly on the metallic Ni(111) substrate and are surrounded by the (7 × 7) wetting layer. This in contrast to the wetting layer of Bi on Si(111), where the semiconducting substrate is first passivated by the wetting layer before electronic growth starts [7,14]. We emphasize that a careful

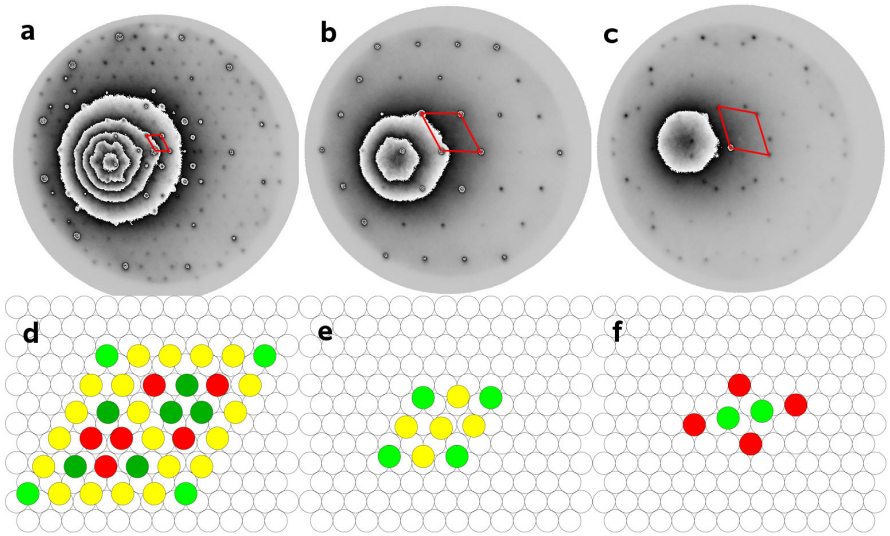

FIG. 2 (color online). μ-LEED images taken at 40.0 eV (a)–(c), and the corresponding real space unit cells (d)–(f) for the three different Bi film structures. Panels (a) and (d) show a (7 × 7) film structure with lattice constant 3.49 Å ($\theta = 0.510$ ML), measured at 422 K. (b) and (e) show a (3 × 3) overlayer with lattice constant 3.74 Å ($\theta = 0.444$ ML), and (c) and (f) show a [3-112] overlayer with a lattice constant 3.80 Å ($\theta = 0.429$ ML), both measured at 474 K. For the real space images (d)–(f) green (dark gray) corresponds to (close to) threefold hollow, red (dark) to (near) on-top, yellow (light gray) to intermediate positions, where in all cases only the contact layer with the Ni(111) surface is drawn.

inspection of the I/V-LEEM data on different (20×20) pixels sized spots across identical domains confirms a very high degree of uniformity and thus indicates constant heights for a particular domain. This is further corroborated by the evolution of the various fractional coverages during deposition. With the numbers given above we obtain a perfect agreement of the previously determined deposition rate and the total coverage as a function of time (see supplemental material [15]). To confirm the origin of the anomalous growth, electron reflectivity curves were measured for both domains as a function of electron energy; see Fig. 3. Quantum-size oscillations are observed for both domains.

For the (3×3) domains two quantum interference peaks are found, whereas for the [3-112] we find four, confirming the previously measured heights. The structure and morphology of Bi films on Ni(111) therefore appears to be almost exclusively determined by QSE.

During experiments at a slightly lower temperature of 422 K a third film structure of type (7×7) was observed,

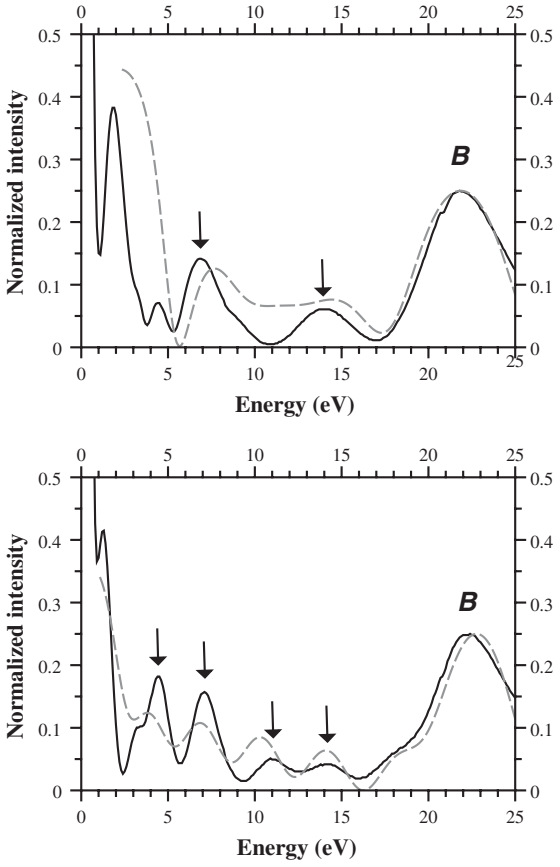

FIG. 3. Quantum interference peaks in I/V-LEEM measurements as indicated by the arrows: two for the three atomic layer high (3×3) (top) and four for the five atomic layer high [3-112] Bi films on Ni(111) (bottom). Experimental curves (black) and best-fit (grey dashed) using the KP model. The Bragg peak at about 22 eV is indicated by B. For the used parameters see Table I.

which was found completely surrounded by (3×3) domains. A height of 7 layers was derived from the growth rate. All μLEED patterns and their corresponding real space unit cells are shown in Fig. 2.

To establish whether $n/2$ times the Fermi wavelength can be accommodated by the three film structures, the interlayer spacings have to be accurately measured. To achieve this, we compare the specular beam intensity to tensor LEED calculations since this peak contains the required information (interlayer distance) most directly. It is in fact the only possible way to determine the interlayer spacing in our instrument. We also note that all μLEED patterns shown in Fig. 2 are sixfold symmetric. This indicates that the domains are in hexagonal AB stacking, as is also found for Bi on Si(111)-(7×7) [7]. In spite of the uncertainties caused by the limited reliability of the used electron-matter interaction potential at very low energies, good quantitative information was obtained. I/V-μLEED curves were calculated using the Erlangen tensor LEED package TENSERLEED [16], where phase shifts were calculated using the EEASISSS package [17]. We have restricted our analysis to the energy window 20–100 eV. The lower limit is determined by the complexity of the electron solid interaction potential at low energies [18,19]. The upper limit is determined by the S/N ratio in our μLEED data. Despite the fact that the calculations were restricted to a simplified geometrical structure that does not take into account any relaxation and no fitting was performed, the Pendry R factors quantifying the comparison are reasonable: 0.136, 0.174, and 0.241 for, respectively, the (3×3), the [3-112], and the (7×7) domains. A clear trend is found when comparing the experimental values with the calculated curves. This leads to a best-fit for the interlayer distance of 3.21 Å for the (3×3) structure, 3.02 Å for the [3-112] structure and, 2.90 Å for the (7×7) structure.

Using these calculated best-fit interlayer distances, a simple Kronig Penney (KP) model was used to model the QSE, see Ref. [20] for a full description. In short: The KP-model uses two potential boxes for each layer, with depth V and width w, centered at the atoms (V_a, w_a) and in between the atoms (V_g, w_g). The substrate is given as a featureless box with depth V_{0s}. By requiring the wavefunctions and their first derivatives to match at the various transitions, including the vacuum-film interface, we can derive the reflection coefficient at the latter interface, which represents the measured quantity. The result is N-1 interference peaks for a N layer thick film.

A good fit (see grey curves in Fig. 3) is obtained using the parameters given in Table I. In both curves the peaks at around 1.8 and 4.4 eV for (3×3) and 1.3 and 3.5 eV for [3-112] are likely a result of the band structure of Bi on Ni(111). For the thicker (7×7) structure the band structure and Bragg peak dominate the I/V-LEEM curve.

TABLE I. Parameters as defined by Ref. [20] used for the KP model fits to the data points shown in Fig. 2. V_{0s} changes for the film structures since it represents the substrate to first layer potential.

Structure	V_a (eV)	V_g (eV)	V_{0s} (eV)	w_a (Å)	w_g (Å)
(3×3)	18.0	4.9	15.0	1.67	1.50
[3-112]	20.7	10.2	20.0	1.34	1.70

Using the best-fit interlayer distances from tensor LEED calculations, we can now find the number of Fermi wavelengths that all three different film structures accommodate. The height of the (3×3), [3-112] and (7×7) domains perfectly accommodate 2.5, 4.0, and 5.5 Fermi wavelengths (see Table II), as calculated using the free electron model taking into account the different electron densities. The interlayer distances from tensor LEED calculations deviate less than 2.5% from the interlayer distance calculated from the free electron model (see row $\Delta a_{\text{inter}}/a_{\text{inter}}$ in Table II). The small mismatch between a perfect $n/2$ times the Fermi wavelength and the height calculations from experiment are perfectly within the error bar of the comparison between tensor LEED calculations and the measured I/V-μLEED curves. For the higher film structures the error is reduced even further, well below 1%. The relaxation d_{12} found for the first layer spacing in QSE-stabilized Pb films [21] is of the order of a few percent, larger than expected for fcc(111) surfaces. Although the d_{12} relaxation plays a lesser role because of the larger mean free path at low energies, it may still contribute to the observed differences. We also note that a mismatch this small could in principle also originate from small phase shifts or other mechanisms that energetically stabilize certain film structures. The different film structures could give rise to small phase shifts, as has been observed experimentally [7]. From these results we can conclude that the free electron model can be used as a valid description for this system. The structural distortion along the trigonal axis is reduced for these three film structures in comparison to bulk Bi. This will result in changes in the band structure as mentioned before. The energetic preference to accommodate the Fermi wavelength in the (7×7) film structure is in fact so strong, that the density becomes even higher than what is known for bulk Bi [6] (see also row labeled density in Table II). The growth of thin Bi films on Ni(111), the quantized heights and film structures, can therefore be identified as almost exclusively determined by the QSE.

TABLE II. Properties of the three different film structures found: in-plane lattice constant (a_{nn}), interlayer distance derived from tensor LEED calculation (d_{TL}), density (ρ), fitted number of Fermi wavelengths, and calculated deviation from interlayer distance as compared to tensor LEED calculation.

Structure	(3×3)	[3-112]	(7×7) [a]
a_{nn}	3.74	3.80	3.49
h(layers)	3	5	7
d_{TL} (Å)	3.21	3.02	2.90
ρ (atoms/nm^3)	25.79	26.48	32.69
$\#\lambda_F$	2.5	4.0	5.5
$\Delta a_{\text{inter}}/a_{\text{inter}}$	2.2%	1.7%	$<1\%$

[a]Measured at 422 K.

In summary, we have presented LEEM and μLEED measurements illustrating *in situ* the QSE driven growth of thin Bi film structures on Ni(111). The measured I/V-LEEM curves show well-defined quantum-size oscillations, that are in agreement with the results of a simple KP model. Three different film structures [(3×3), [3-112], and (7×7)] grow at specific heights of 3, 5, and 7 atomic layers. Comparing tensor LEED calculations to I/V-μLEED curves we are able to calculate the height of these film structures, which perfectly accommodate $n/2$ times the Fermi wavelength and thereby illustrate the relevance of the QSE for quantization of island heights and ultimate film structure.

This work is part of the research programme of the Foundation for Fundamental Research on Matter (FOM), which is financially supported by the Netherlands Organization for Scientific Research (NWO). T. R. J. B. thanks John Rundgren and Christina Ebensperger for useful discussions.

[1] S. Yaginuma, K. Nagaoka, T. Nagao, G. Bihlmayer, Y. M. Koroteev, E. V. Chulkov, and T. Nakayama, J. Phys. Soc. Jpn. **77**, 014701 (2008).
[2] Z. Zhang, Q. Niu, and C.-K. Shih, Phys. Rev. Lett. **80**, 5381 (1998).
[3] K. Budde, E. Abram, V. Yeh, and M. C. Tringides, Phys. Rev. B **61**, R10 602 (2000).
[4] M. Hupalo and M. C. Tringides, Phys. Rev. B **65**, 115406 (2002).
[5] M. M. Özer, C.-Z. Wang, Z. Zhang, and H. H. Weitering, J. Low Temp. Phys. **157**, 221 (2009).
[6] N. W. Ashcroft and D. N. Mermin, *Solid State Physics* (Thomson Learning, Toronto, 1976), 1st ed., ISBN 0030839939.
[7] T. Hirahara, T. Nagao, I. Matsuda, G. Bihlmayer, E. V. Chulkov, Y. M. Koroteev, and S. Hasegawa, Phys. Rev. B **75**, 035422 (2007).
[8] K. Gürtler and K. Jacobi, Surf. Sci. **152–153**, 272 (1985).
[9] M. Ondrejcek, M. Rajappan, W. Swiech, and C. P. Flynn, Phys. Rev. B **73**, 035418 (2006).
[10] K. Umezawa, A. Takahashia, T. Yumuraa, S. Nakanishia, and W. M. Gibson, Surf. Sci. **365**, 118 (1996).
[11] K. Umezawa, S. Nakanishi, T. Yumura, W. M. Gibson, M. Watanabe, Y. Kido, S. Yamamoto, Y. Aoki, and H. Naramoto, Phys. Rev. B **56**, 10 585 (1997).
[12] D. Brown, P. D. Quinn, D. P. Woodruff, P. Bailey, and T. C. Q. Noakes, Phys. Rev. B **61**, 7706 (2000).

[13] The Bi nanowires grow in threefold symmetric directions as well as with a 22° rotation on that. μLEED measurements show matrix structure ($m_{11} = 2$, $m_{12} = 0$, $m_{21} = -2$, $m_{22} = 5$) ordering; T. R. J. Bollmann, R. van Gastel, H. J. W. Zandvliet and B. Poelsema, Phys. Rev. B (to be published).
[14] T. Nagao, T. Doi, T. Sekiguchi, and S. Hasegawa, Jpn. J. Appl. Phys. **39**, 4567 (2000).
[15] See supplemental material at http://link.aps.org/supplemental/10.1103/PhysRevLett.107.176102 for details.
[16] V. Blum and K. Heinz, Comput. Phys. Commun. **134**, 392 (2001).
[17] J. Rundgren, Phys. Rev. B **68**, 125405 (2003).
[18] J. Sun, J. B. Hannon, G. L. Kellogg, and K. Pohl, Phys. Rev. B **76**, 205414 (2007).
[19] K. Heinz (private communication).
[20] M. S. Altman, W. F. Chung, and C. H. Liu, Surf. Rev. Lett. **5**, 1129 (1998).
[21] A. Mans, J. H. Dil, A. R. H. F. Ettema, and H. H. Weitering, Phys. Rev. B **72**, 155442 (2005).